NRIAG JOURNAL OF ASTRONOMY AND GEOPHYSICS
2020, VOL. 9, NO. 1, 512–531
https://doi.org/10.1080/20909977.2020.1788270

Investigation of groundwater occurrences in structurally controlled terrain, based on geological studies and remote sensing data: Wadi El Morra, South Sinai, Egypt

Hussien M. Hussien[a], Mohamed Yousif[a] and Abdelfatah El Sheikh[b]

[a]Geology Department, Desert Research Center, Cairo, Egypt; [b]Hydrology Department, Desert Research Center, Cairo, Egypt

ABSTRACT

The investigations of groundwater occurrences and its recharge mechanisms in structurally controlled terrain under arid environments are necessary for developing sustainable management strategies. In current study, an interdisciplinary approach includes readily accessible climatic, geological, topographic, and hydrological datasets together with satellite imagery and field data, were employed for better understand of the groundwater regime existing under special geological setting. Our findings indicate that: 1) the Araba sandstone aquifer has maximum thickness of about 220 m in some area controlled by structural setting, particularly the basement uplift, 2) the hydrologic analyses of this basin revealed that it received a total 52.66×10^6 m^3 of rainfall between July 2018 to June 2019 that led to runoff volume about 29.47×10^6 m^3 with total losses amounts about 23.2×10^6 m^3, 3) topographically-driven modern recharge to the structural controlled terrain (Wadi El Morra) can be occurred, and therefore further investigation related to the aquifer response to climate variability, are required. The study suggested a management plan to capitalize the available surface water potentialities of El Morra basin through establishing three lakes that store water and enhance the groundwater recharge opportunities. In addition, three regions are selected for future groundwater exploration based on geological and subsurface data.

KEYWORDS

Geology; groundwater; hydrology; remote sensing; Sinai; Egypt

1. Introduction

Development plans in arid and semi-arid regions relies on the availability of water resources (i.e. groundwater and surface water) and their proper management. Arid and hyper-arid regions (e.g. Sinai Peninsula and the Eastern Desert of Egypt) are suffering mostly from the scarcity of fresh water supplies. However, Sinai Peninsula is classified as an arid zone (UNESCO 1979) and its water resources are very limited, it is frequently subjected to heavy storms, which produce flash floods (Moawad 2013). These flash floods are consider very important source of fresh water for the locals and additionally enhance the recharge of the shallow groundwater aquifer (Hussien et al. 2017; Yousif and Hussien 2020). The hydrogeological condition in El Morra basin is highly controlled by many factors such as climatic conditions, geological and structural settings. As a part of Sinai Peninsula, Wadi El Morra basin is subjected to several structural features (e.g. shear zones, uplift, faults and fractures), which are attributed to the Pan African orogeny in late Proterozoic (Bentor 1985; Loizenbauer et al. 2001) as a part of the Arabian Nubian shield. Despite of the structural controls in El Morra basin, a comprehensive understanding of the effect of structural control on groundwater occurrences is poorly constrained. As a result, four dry groundwater wells have been drilled in the study area due to the in proper selected sites that are neglected the impact of structural setting. In order to conducting a comprehensive watershed analysis in addition to investigating the hydrogeological setting in the study area, it is necessary to understand structural settings, topography, erosion status and drainage patterns of the region (Solomon and Quiel 2006; Sarikhani et al. 2014). Generally, the interpretation of the satellite images (e.g. Landsat-8 and Shuttle Radar Topography Mission [SRTM]) jointly with the geophysical data (e.g. Vertical electrical sounding data) provide valuable information about the geological and topographic settings especially in arid environments (Sultan et al. 2011; Mohamed et al. 2015). Moreover, the data acquired from the geophysical investigations (e.g. vertical electrical sounding) is considered as important tool in detecting hidden subsurface structures (Muchingami et al. 2012; Adagunodo et al. 2013). In this manuscript, the authors adopt an interdisciplinary approach which includes readily accessible climatic, geological, topographic, geophysical and hydrological datasets of El Morra basin, together with satellite imagery as well as field data to investigate the groundwater occurrences and estimates the rainfall/runoff relation in structurally controlled terrains under arid condition. Finally, a proper management plans was suggested to maximise the beneficiary of surface runoff

CONTACT Mohamed Yousif yousif_mohamed80@daad-alumni.de Geology Department, Desert Research Center, Cairo, Egypt

and groundwater potentiality in El Morra basin. Additionally, suggesting some suitable sites for exploring high potential groundwater wells.

2. Site description

Wadi El Morra is located at the upstream portion of one of the most famous basins in south Sinai Peninsula, Wadi Dahab, which follow the Gulf of Aqaba Hydrographic basins (Omran et al. 2011) (Figure 1). It lies along the asphaltic road connecting between Nuweiba and Saint Katherine where its measured surface area is about 243 km^2. Geomorphologically, Wadi El Morra is an ephemeral drainage network collects sporadic rainfall from watersheds draining the northern and southern highlands and sporadically it receives intermittent flash floods events (Alnedawy et al. 2015; Yousif and Hussien 2020). The plain area of the basin is covered by washed and drift sands that underlain by the sandstone of Araba Formation. The interaction between the tectonic evolution, the weathering and erosion processes ultimately led to the present major geomorphological features in the study area including; the basement terrains, the alluvium plain, the sedimentary blocks, and the isolated hills (Figure 2). Along Wadi El Morra basin, several lithologic units are ranging, in age, from Pre-Cambrian to Quaternary are exposed (Figures 3 and 4). The Pre-Cambrian fractured basement is mainly of Late Proterozoic age. These rocks consist mainly of igneous and metamorphic rocks, which underlain a thick succession of Sandstone, Shale, Limestone of Cambrian to Cretaceous ages and finally topped by Quaternary alluvium deposits (Klitzsch et al. 1987; Said 1990). These successions include (from base to top) the Araba and Naqus Formations of Cambrian age, Raqabah Formation of Jurassic age, Malha Formation of Albian-Aptian age, Galala Formation of Cenomanian, Wata Formation of Turonian age and finally Quaternary alluvium deposits (Klitzsch et al. 1987). Araba Formation is considered the main water bearing formation in the study area (Hasanein 2007). It is composed of thick-bedded (130 m) medium to fine-grained sandstone with iron oxides and clay sheet intercalations (Shabana 1999). This formation is unconformably underlies the Quaternary deposits at plainly areas of the main stream of Wadi El Morra (Al-Abaseiry and Al Temamy 2012). Structurally, Southern Sinai is strongly influenced by the Red Sea rifting, Gulf of Suez (NW-SE trend) and Gulf of Aqaba (NNE-SSW trend) where many faults are formed during their developments (Said 1990; Sharp et al. 2000; Arnous and Sultan 2014). During the tectonic development of the Gulf of Aqaba Rifting system, a shear belt of sub parallel faults, 30 km width, was developed along the western coast of the Gulf of Aqaba (Eyal et al. 1981). This shear belt which trending N-S to NE-SW was observed mainly within the Pre-Cambrian basement terrain. As a part of this structural setting, Wadi El Morra basin forms a morphotectonic depression trending NW-SE in which exploration for the groundwater is a vital element (Hasanein 2007). Accordingly, the identification of these

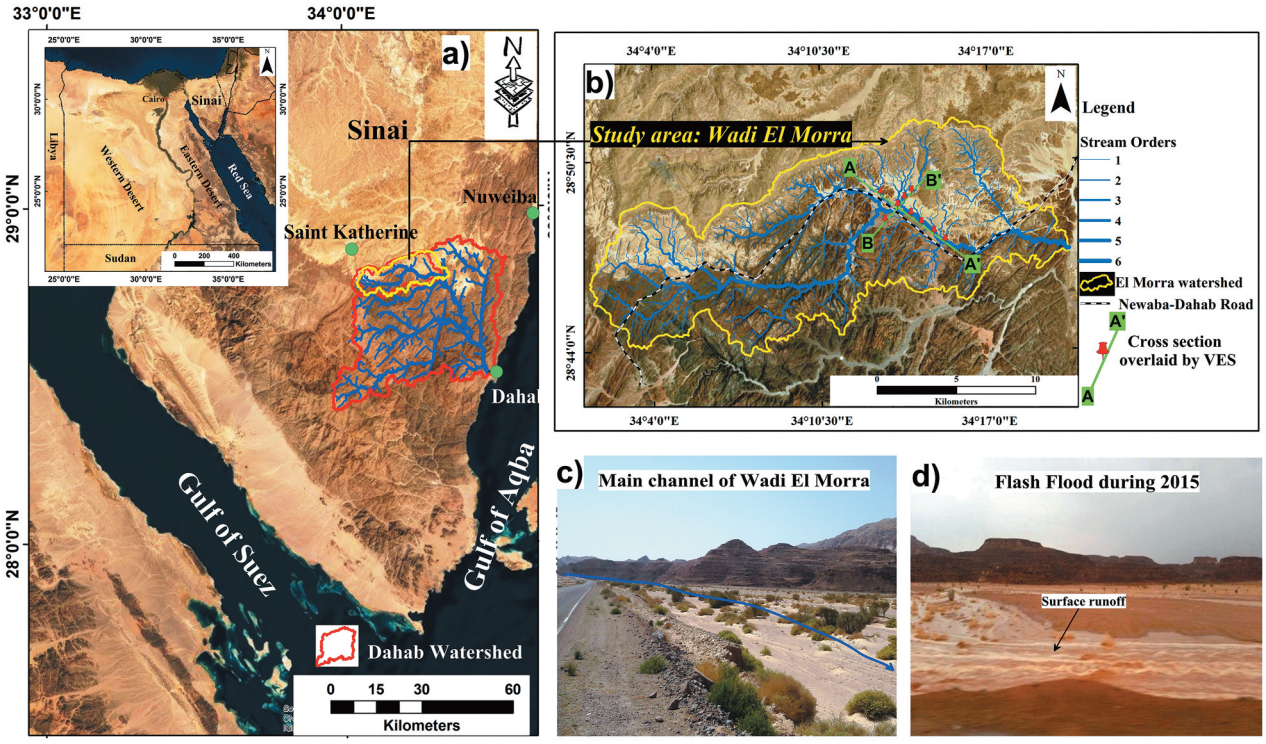

Figure 1. (a) Regional map of Sinai showing the geographic location of the study area; (b) a close up view of the studied basin with illustration of the two cross sections locations and catchment boundary of El Morra basin; (c, d) Field photos showing the main channel of El Morra basin and flash floods during 2015, respectively.

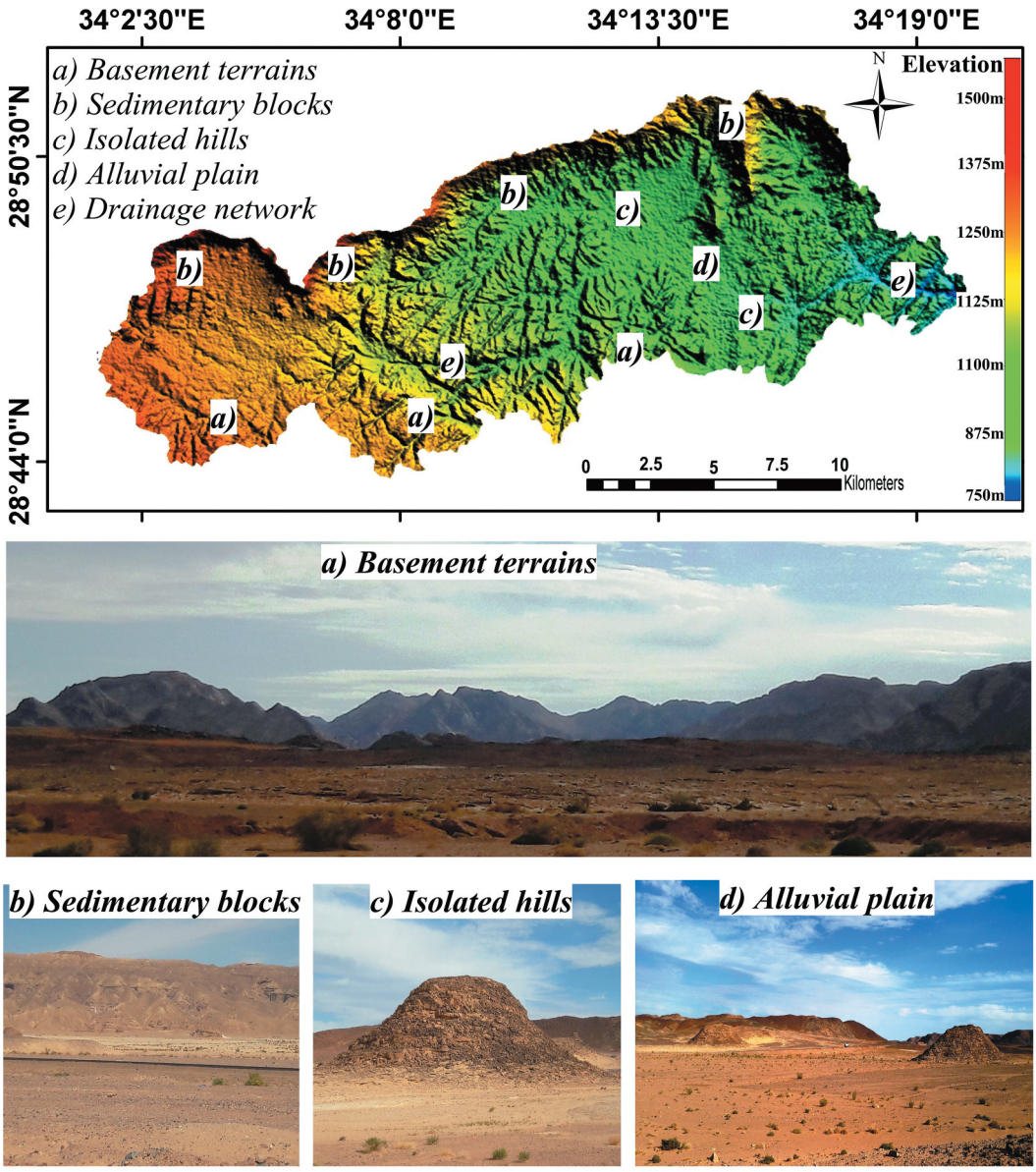

Figure 2. Digital elevation model (DEM) of El Morra basin with the locations of the main geomorphologic units, supported by field photos (a–d) illustrate these units.

structure features is a significant point in the hydrogeological investigations of the area, since they characterise areas of high infiltration capacities and good groundwater potentiality. The Araba Formation is the main water bearing Formation in Wadi El Morra basin. It is recharged by flash floods when the basin receives heavy storms and infiltration of precipitation occur (El Rayes 1992; JICA, 1999).

3. Materials and methods

3.1. Field work

Fieldwork have been conducted in March 2019 as a part of the hydrogeological investigation for the desert areas in Sinai Peninsula which leaded by the Desert Research Centre in Cairo. Several sites were checked in details in order to identify the geomorphological, geological and structural settings of these locations. The field data was used in area-wide interpretation as well as the verification of the outputs and the results of the analysed satellite images. Hydrogeological survey of the existing groundwater wells was carried out in Wadi El Morra basin. A Garmin global positioning system (GPS) model eTrex 10 was used to define the location of 11 water point tapping, the Araba sandstone Formation, the main aquifer in the study area. Also, the locations of the measured surface sections were identified. Unfortunately, because of the sealing of the water points only three water samples were collected. The pH-values and electrical conductivity (EC) of the collected samples were measured onsite. Ultimately, the depth to groundwater, the water bearing formation type and the total depth of the water wells were identified.

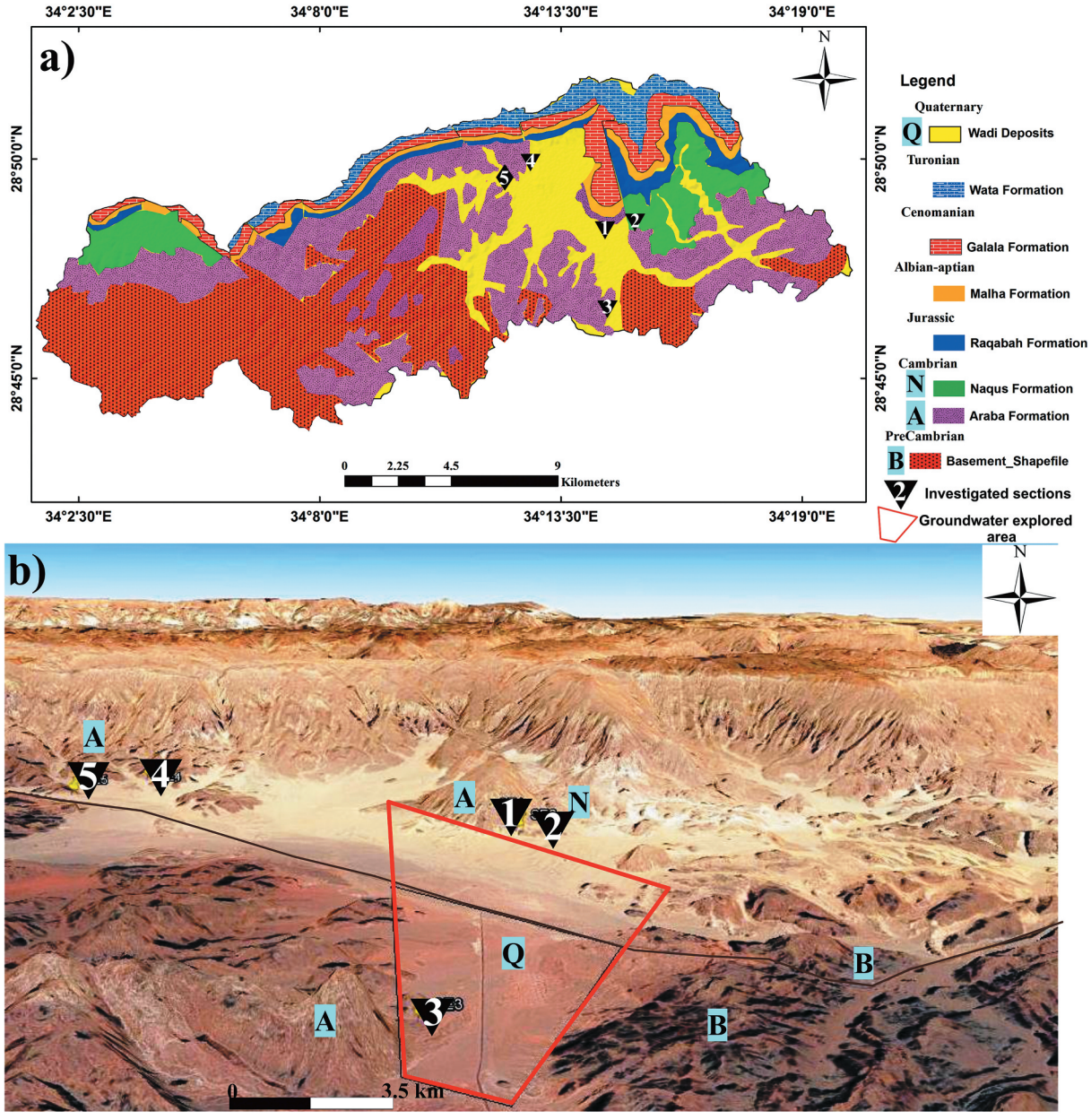

Figure 3. (a) Geological map of the studied basin (Klitzsch et al. 1987) display the main rock units. Also, shown are the locations of the measured surface sections (1–5). (b) 3D view showing the current explored area with the geological exposures.

3.2. Remote sensing and geographic information system (GIS) Data

The remote sensing data sets [Landsat 8 (LC8), Digital elevation model (DEM), Google earth view, Vertical electrical sounding (VES)] provide the basic information in the present study. So, The Shuttle Radar topographic mission DEM with Landsat 8 was used in visual interpretations of the main topographic features and identifying the main geomorphologic units in the study area. Furthermore, the Hillshade relief map which derived from SRTM DEM (spatial resolution, 30 m) was used with Landsat 8 image in Arc GIS environment to extract the linear features (faults and/or fractures) in El Morra basin. The structural lineaments were traced manually from the created Hillshade layer and then were used to identify the main structural trends in the study area. For additional correlation process, all the collected data (DEM, LC8, geologic maps, topographic maps) are registered to unified projection Universal Transverse Mercator (UTM) zone; 36 North with WGS84 datum in GIS environment. All the remote sensing data were obtained using the website[1] of the United States Geological Survey (USGS). The Landsat 8 ratio image (e.g. 4/3, 6/2 and 7/4 in RGB) were created. The ratios of bands 4/3, 6/2 and 7/4 in LC8 are characteristic ratios for lithological differentiation between various rock types based on their chemical and mineralogical compositions. These ratios were used in geological mapping as well as visualising interpretation of structural lineaments in

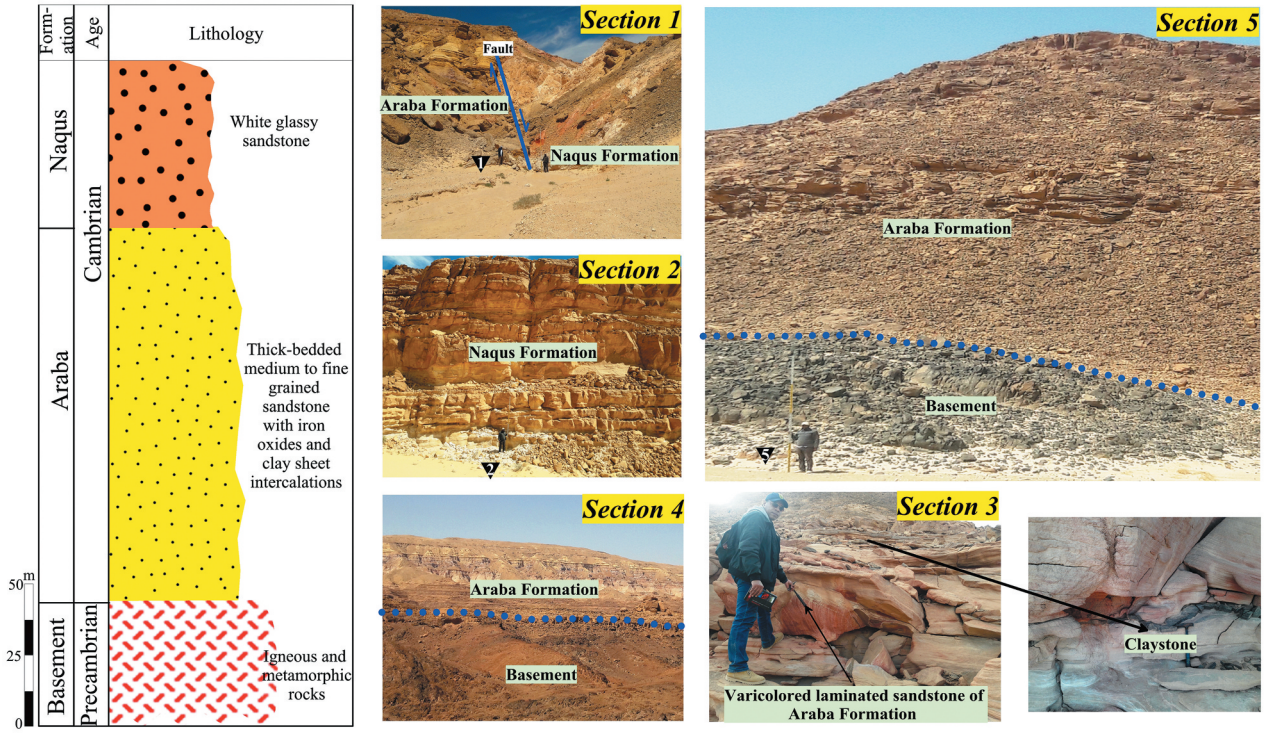

Figure 4. Composite stratigraphic section of the study area with field photos of the studied basin showing the measured sections (sections 1–5) with their stratigraphic formation, sedimentary structures and tectonic elements.

semi-arid to hyper-arid region (Yousif and Hussien 2020). Moreover, DEM was used in extracting the watershed boundaries as well as the drainage network of El Morra basin, where the D8 flow direction algorithm is used in Arc GIS hydro program which described by (O'callaghan and Mark 1984). Also, the slope layer of the study area was created from the DEM using the Arc GIS program.

3.3. Chemical analysis

Three groundwater samples tapping the Araba Sandstone Formation were collected for chemical analysis which includes major and trace elements. Total alkalinity (HCO^{3-} and CO_3^{2-}) was measured using the potentiometric titration method that illustrated by Fishman and Friedman (1985). The concentration of the major anions and cations are measured using Ion Chromatography (IC) (Dionex ICS-1100) at Desert Research Centre, Cairo, Egypt, while, trace elements (Fe, Cu, Zn, Mn, Cd, Mo, Pb, Cr, Ni, NO_3, P_2O_5) were measured using Atomic Absorption Spectrometry (AAS).

3.4. Stream power index (SPI)

SPI is introduced by Moore et al. (1991) where it measures the erosive power of the flowing water and in general it is topographically controlled compound. The stream power index is calculated using the following formula;

$$SPI = As \times \tan \beta \quad (1)$$

Where, *As* is the upslope contributing area and β is the topographic gradient (slope) measured in degree. In general, DEM is the starting layer used in Arc GIS software to extract the slope and flow accumulation in order to get the final values of SPI, in raster format, according to the abovementioned formula.

3.5. Topographic wetness index (TWI)

TWI is an index introduced by Beven and Kirkby (1979) which consider as an indicator about the effect of local topography on the runoff flow direction as well as the accumulation of rainfall. The equation used to calculate the TWI at a certain point is defined as follow;

$$TWI = \ln\left(\frac{As}{\tan\beta}\right) \quad (2)$$

Where, *As* is the upslope contributing area and β is the topographic gradient (Slope). The values of TWI are automatically calculated using the SRTM DEM of the study area in Arc GIS environment. Where, flow direction, flow accumulation, and slope are the most important derivatives of the DEM which used in calculating TWI. The end result is GIS data layer (raster) that describes areas with drainage depressions where water is probable to accumulate. The value of each raster is relative within the specific study area.

[1](http://www.earthexplorer.usgs.gov).

3.6. Rainfall analyses

The rainfall data was downloaded from the Global Rain Map (GSMAP) website which was developed by the JAXA Global Rain Water Watch System (Ver. 4.0) of the Earth Observation Research Centre of Japan, where six events were observed through the hydrological year (July 2018 to June 2019). These data were used to develop the hydrographs of the studied watershed of El Morra basin.

3.7. Estimation of rainfall/surface runoff relationship

To estimate the rainfall/runoff relation of El Morra basin, the Soil Conservation Service (SCS-CN) method (SCS, 1972) was applied. The SCS-CN method was originally designed for agricultural catchments in the United States, and has since been adapted to measure infiltration losses in arid areas of Saudi Arabia and the United States (Graf 1988; Walters, 1990) with similar climatic and physiographic conditions. This relation is very important in watershed management schemes, applied to sustain the water resources in both flood and drought periods. The SCS runoff curve number method is used to model the hydrographs at each subcatchment outlet, relating hydrograph characteristics (lag time, peak discharge, base time, etc.) to catchment parameters (area, length, hydrological characteristics, soil cover types) (Masoud 2011). The SCS-CN method is based on the principle of the water balance and two fundamental hypotheses. The first hypothesis states that the ratio of direct runoff to potential maximum runoff is equal to the ratio of infiltration to potential maximum retention. The second hypothesis states that the initial abstraction is proportional to the potential maximum retention. The water balance equation and the two hypotheses are expressed mathematically as follow:

$$P = I_a + F + Q \tag{3}$$

$$Q/(P-I_a) = F/S\ I_a = DS \tag{4}$$

Where: P is the total precipitation (mm), I_a is the initial abstraction before runoff (mm), F is the cumulative infiltration after runoff begins (mm), Q is direct runoff (mm), S is the potential maximum retention (mm), and λ is the initial abstraction (ratio) coefficient. To minimise uncertainty in the determination of the storm event discharge, storms events with $P \geq 5$ mm have been considered to determine CN values in calibration period (Manoj and Dholakia 2014). In validation period all events have been considered to measure performance of different procedures. A value of $\boldsymbol{\lambda} = 0.2$ was assumed in original SCS-CN model. The general runoff equation combination of Equation (3) and Equation (4) is shown in Equation (5):

$$Q = (P-I_a)^2/P-I_a + S \text{ For; } P > I_a \tag{5}$$

The potential maximum retention S (mm) can vary in the range of $0 \leq S \leq \infty$, and it directly linked to CN. Parameter S is mapped to the CN using Equation (6) as follow:

$$S = (25400/CN) - 254 \tag{6}$$

The CN depends on the hydrological soil group, antecedent moisture condition (AMC) and hydrologic conditions and it may vary from 0 to 100. The hydrological soil groups are discriminated into four groups. Group A has a high rate of water transmission and describes the soil which consists of deep well to excessively well-drained sands or gravels. Group B consists chiefly of moderately fine to moderately coarse textures that have a moderate rate of water transmission. Group C describes fine to fine texture soils that have a slow rate of water transmission. On the other hand, group D describes soils which consist of clay with high swelling potential, high-water table, clay layer near the surface, rocky basement areas and shallow soils over nearly impervious material. These soils have a very slow rate of water transmission. Antecedent Moisture Condition (AMC) refers to the water content present in the soil at a given time. Three AMCs were defined as dry (lower limit of moisture or upper limit of S), moderate (normal or average soil moisture condition), and wet (upper limit of moisture or lower limit of S). The third parameter is the hydrological conditions which measure how dense the land cover. Three types are characterised; poor (less than 50% land cover), fair (moderate cover), good (heavy/dense land cover). The weighted CN is applied for the basins of many soil types as follow equation (7)

$$\mathrm{CN_W} = \Sigma A_i CN_i/\Sigma A_\mathrm{i} \tag{7}$$

Where; $\mathrm{CN_i}$ is the CN for a part of the watershed of an area A_i.

3.8. The hydrological model "HEC-HMS"

The hydrological model "HEC-HMS" version 3.5 is used to simulate the hydrological condition of the studied basin and generate the watershed hydrograph (HEC-HMS 2010). This software is designed to simulate the precipitation/runoff response of a wide range of watersheds. The rainfall data was collected from six storms precipitated in the hydrologic year 2018–2019. They were used as input data in the meteorological model of the HEC-HMS program. These data include the beginning and the end time of the storm, duration in hour and rainfall intensity in mm/hr. El Morra catchment area (243 km^2) was subdivided into

three sub-basins. Junction-1 represents the collection point of the excess rainfall from subbasin-1 and subbasin-2. Runoff water flows from this point through reach-1 to the outlet point (Junction-2) which represents the basin's outlet where runoff water from reach-1 and subbasin-3 is collected (as it will be shown later in Figure 11). The model input data includes the rainfall data, physical watershed parameters (basin, sub basins, areas, reaches and outlet). Hydrological parameters; i.e. initial abstractions (Ia), curve number (CN), slope, impervious ratio, time of concentration (T_c) and lag time (T_L). The time of concentration (T_c) is defined as the travel time in minutes for a drop of water to travel from the hydraulically most distant point of the watershed to the gauging point downstream (Chow et al. 1988). The Kirpich (1940) formula was used to estimate the value of the time of concentration of every sub-basin. This formula is a popularly used formula relating the time of concentration of the length of travel and slope of the catchment as follow:

$$T_c = 0.0078L^{0.77}S^{-0.385} \quad (8)$$

Where T_c is time of concentration (minutes); L is maximum length of travel of water (km) and S is slope of the catchment (m/Km). On the other hand, the lag time is the difference in time between the centre mass of the net rainfall and centre of mass runoff. The lag time (T_L) is about 0.6 T_c according to the SCS method. Routing the watershed is the final step in generating the basin hydrograph. Routing is the movement of the runoff from the different watersheds outlets throughout the system along the stream, and ultimately to the outlet or sink of the entire watershed system (Chow et al. 1988). The HEC-HMS model routing options include the Muskingum, Modified Plus, Kinematic Wave, and Muskingum-Cunge methods.

3.9. Estimation of runoff coefficient

The runoff coefficient is the relation between the runoff depth and rainfall depth, which represent the amount of rainfall transmitted to runoff. The runoff depth and runoff coefficient are calculated using the following equations (Ponce 1989):

$$\text{Runoff depth (mm)} = \text{Runoff volume}/\text{Drainage area} \quad (9)$$

$$\text{Runoff coefficient (\%)} = \text{Runoff depth}/\text{Rainfall depth} \quad (10)$$

4. Results

4.1. Lithologic discrimination

In the current study, five geological sections were measured where the total thickness is ranging between 35 and 85 m of Araba and Naqus Formations (Figure 3). These sections were selected around the explored area whereas, groundwater wells were imposed to investigate the surface exposures which will be linked with the subsurface succession. The investigated sections reveal that Araba Formation represents the soul aquifer in the area, is consisting of varicoloured Sandstone with rare clay intercalations, characterised by cross bedding, and laminated sedimentary structures. This sandstone is coarse grained, fractured and slightly faulted (Figure 4). The Araba Formation (Cambrian) is overlying the Precambrian basement rocks and overlaid by Naqus Formation followed by Upper Cretaceous succession. The Naqus Formation (Cambrian) is consisting of white glassy fractured sandstone. The investigation of the band ratio thematic layer (Figure 5) clarifies a distinct boundary between the basement "B" uplift in the southern portion of the basin and the sedimentary basin (covered by Araba "A" and Naqus "N") in the northern side. The band ratio calculation discriminates the Quaternary alluvial sediments into two types; Q1: alluvial deposits resulted from sandstone weathering, and Q2: alluvial deposits resulted from basement weathering.

4.2. Structural setting

The geological structures of Southern Sinai can be considered as a part of the Arabian-Nubian Shield which was resulted from many complex events of subduction, accretion and extension throughout Pan African periods (Shimron 1984; El Shafei et al. 1992). The inspections of band ratio image together with geologic maps and field investigation illustrated that the general structure setting of the study area was influenced by the Red Sea rifting (NW-SE trend), Gulf of Suez (NW-SE trend) and Gulf of Aqaba (NNE-SSW trend) where many shear zones were formed during their developments. The extracted structural lineaments (faults and/or joints) of Wadi El Morra show that NE – SW, NNE – SSW and NW-SW are representing the main trends (Figure 6). It is observed from the analysis of these lineaments that most drainage streams are structurally controlled and that they are initiated as a result to the tectonic movements related to the basement uplift and the extension stress. Two shear planes are affected the studied basin, the first is a left lateral strike-slip fault (NE to NNE), while the second is a right-lateral strike-slip fault (NW-SE), (Hegazi 2006). The investigation of band ratios map shows that many dykes are intersecting the basement rocks (Figure 5) with NE-SW trend which is parallel to the Gulf of Aqaba rift.

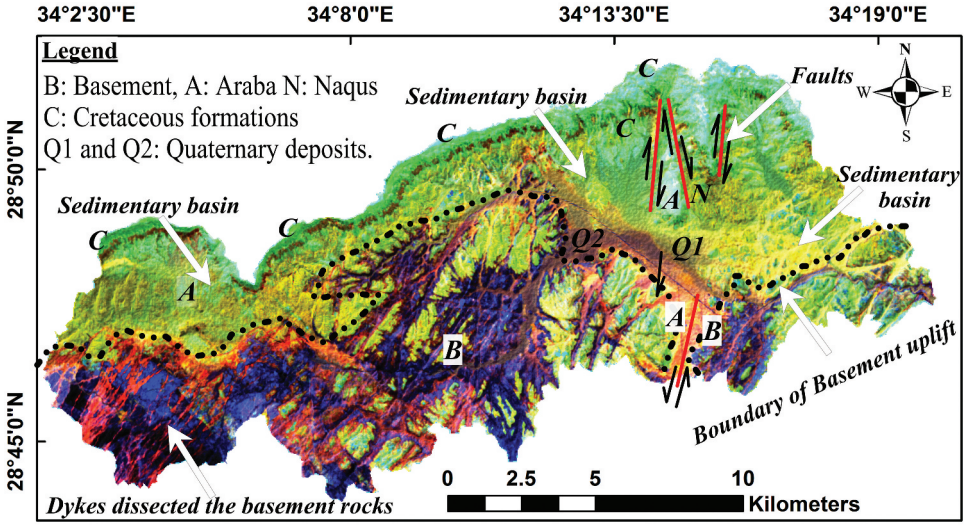

Figure 5. Band ratio image for Landsat 8 for the studied basin shows the northern sedimentary basin (with different geological formation) and the uplifted basement rocks dissected by a group of dykes which trending NE-SW (Aqaba trend).

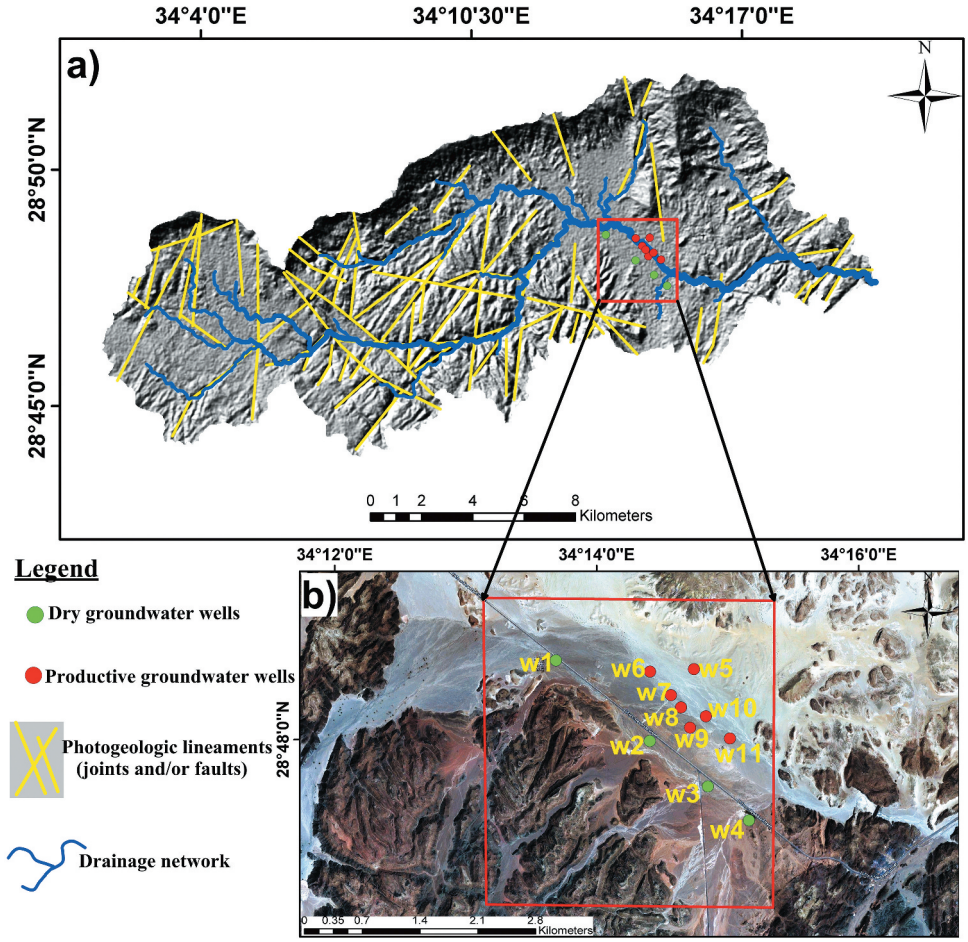

Figure 6. Structural linemants draped over the hill-shaded relief map of El Morra basin illustrate the main structural trends. Also, shown are the spatial distribution of water points. (b) Wells location map where the productive and dry wells are overlaid the landsat 8.

4.3. Hydrogeologic setting

The groundwater occurrence in Sinai is variable from one place to another due to many reasons including structural and geomorphologic settings, subsurface heterogenetic and recharge sources. In the current study, only one aquifer is existed in El Morra basin representing by Araba Formation (Cambrian age) that is belonging to Nubian sandstone aquifer. The lithology of the aquifer is mainly

sandstone with silt and clay intercalations where it is present under semi-confined condition. The spatial distribution of the recorded wells shows that seven productive wells (Wells nos. W6 to W11) penetrate the aquifer while another four dry wells (Wells nos. W1 to W4) are recorded to the south of the main channel (Figures 6(b) and 7). The total penetrated depth of these wells is ranging between 35 m (W4, dry) and 120 m (W11, productive), (Table 1). The groundwater exists under free water table conditions at about 35 m below the ground surface (+845 m above sea level). The subsurface setting was clarified through the lithologic well logs and geophysical data.. This investigation reveals that the Quaternary alluvial show about 30 m sediments, while the Araba Formation has its maximum thickness with about 220 m at VES no.2 (Figure 7(a)). To the south of the main channel, the drilled wells penetrate the dry alluvial deposits with about 14 m and the underlain basement rocks with 70 m (Well no. W2). To illustrate the subsurface setting and the recharge opportunities of the studies basin, two hydrogeologic schematic cross sections were drawn. The first section (A-A') has NW-SE trend and runs along the main channel passing by VES No. six (Al-Abaseiry and Al Temamy 2012) and one well (W7), (Figure 7(a)). It shows that the sandstone of Araba Formation is fully saturated with water where the aquifer can be recharged through the watersheds (basement and sandstones exposures) and direct infiltration from the surface runoff. The second section (B-B') is completed using four VES (Al-Abaseiry and Al Temamy 2012), (Figure 7 (b)). This section is confirming the same conceptual model about the recharge sources as it was explained in section A-A'. Both cross sections approved the existence of 10 faults on local scale where these faults also can contribute positively in groundwater recharge through surface-groundwater interaction. From the productive wells, three wells are operating and pumping water for drinking purposes where they show total dissolved salts (TDS) range between 593 mg/l and 892 mg/l (Table 2). The slight variation of TDS values may be attributed to the remoteness from the recharge areas (foothills of the basement and sandstone exposures). The three analysed groundwater samples show Na-Cl water type, where the ion excess of Cl^- and Na^+ attributes to the joint effect of the ferruginous lamina of sandstone and the dissolution of main watershed terrains (basement). The increase of Ca^{2+} and Mg^{2+} ions could be derived from the dissolution of basement rocks and/or cation exchange of Na^+ with Ca^{2+} and Mg^{2+} above clay minerals (clay is rarely intercalated with sandstone). The obtained trace elements indicate that the groundwater of Araba Sandstone aquifer is suitable for drinking where all concentrations under the permissible levels (WHO, 2014).

4.4. Thematic GIS layers

4.4.1. Slope

Slope is an important factor in watershed analysis, management as well as in identifying the groundwater recharge zones (Yousif and Sracek 2016; Das 2018; Yousif and Hussien 2020). Where, it affects greatly on the runoff speed, runoff retention of soil surface and finally infiltration capacity. The analysis of DEM of El Morra basin has been carried out to identify the slope classes. The slope of the watershed was grouped into five classes as; "Gentle slope" (0–10), "Moderate slope" (10–20), "Moderate Steep slope" (20–35), "steep slope" (35–50) and "Very steep slope" (> 50) (Figure 8(a)). It is obvious that the gentle slops characterising the low laying areas in the basin and along its drainage lines. These flat areas generate very good chance for groundwater recharge capability since they influence high infiltration rates and less generation of surface runoff.

4.4.2. Stream power index

Stream power index (SPI) was supposed to influence the characteristics of soil, distribution, and abundance of soil water, vulnerability of landscape to weathering and erosion by water, as well as the

Table 1. Recorded data of the drilled groundwater wells in Wadi El Morra.

Well no.	Coordinates		Current status	Total depth (m)	Notes (Subsurface and penetrated aquifer)
	Long. (E)	Lat. (N)			
W1	34.227975	28.808597	Dry since drilling	120	Produced 6 m^3 of water on the start only
W2	34.239806	28.799444		84	Drilling for 14 m in alluvial, then penetrates basement rocks
W3	34.247139	28.794278		–	Without information
W4	34.252306	28.790417		35	Drilling in sandstone for 10 m then penetrates basement rocks
W5	34.245528	28.807444	Productive/not working	–	Drilled for Aqua Catherin Co., Penetrates Araba F., closed by company
W6	34.239944	28.807222	Productive/not working	–	Drilled for Aqua Catherin Co., Penetrates Araba F., closed by company
W7	34.242556	28.804556	Productive/working	110	Drilled for Holding Co., Penetrates Araba F., TDS = 593 mg/l, discharge 40 m^3/h
W8	34.243833	28.803167	Productive/not working	–	Drilled for Aqua Catherin Co., Penetrates Araba F., closed by company
W9	34.244944	28.800889	Productive/working	110	Drilled for Holding Co., Penetrates Araba F., TDS = 602 mg/l
W10	34.246972	28.802139	Productive/not working	–	Drilled for Aqua Catherin Co., Penetrates Araba F., closed by company
W11	34.25	28.799639	Productive/working	120	Drilled for local people, Penetrates Araba F., TDS = 892 mg/l

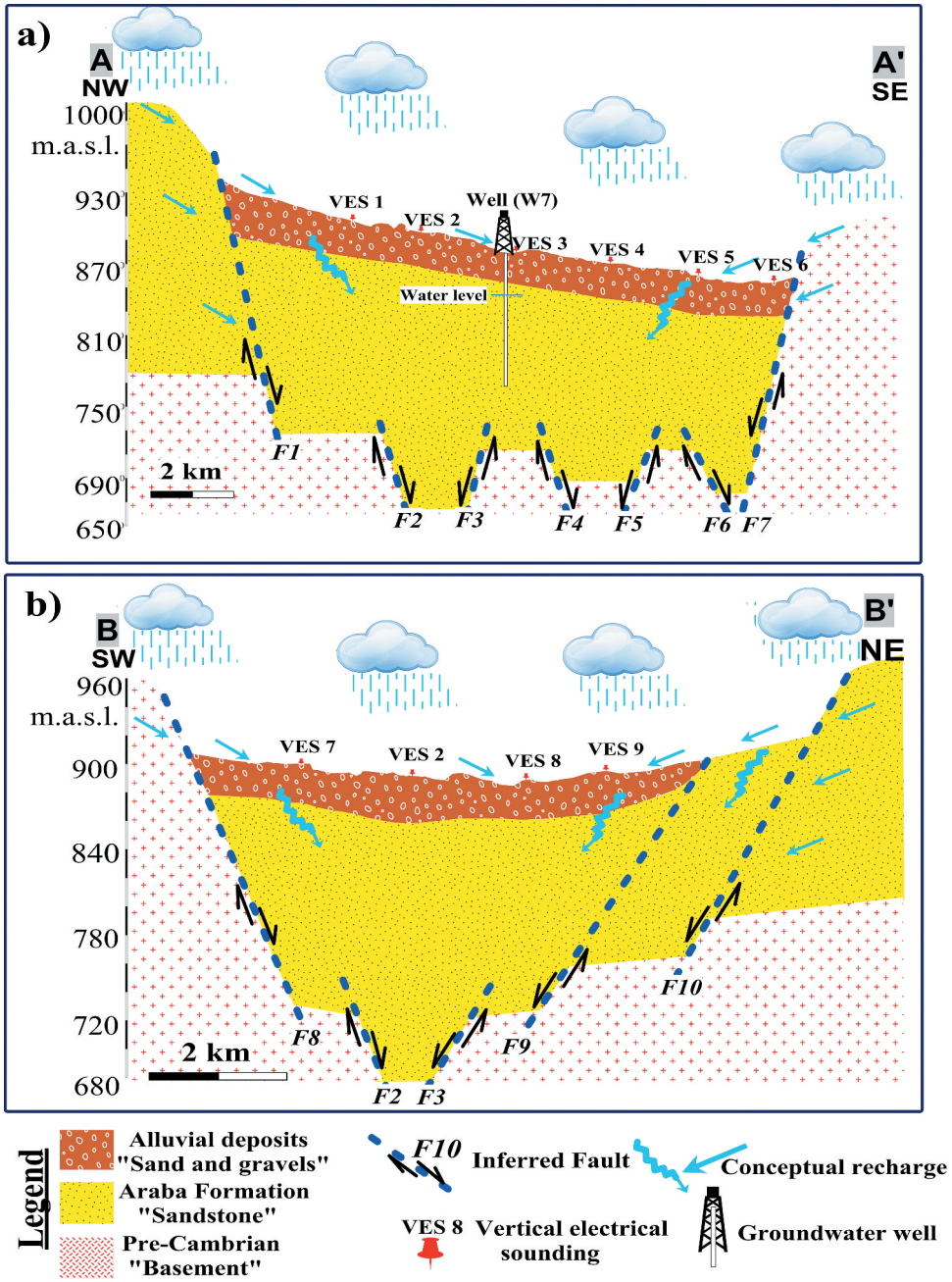

Figure 7. Shows two schematic cross sections (A-A′) and (B-B′) respectively, illustrates the groundwater recharge opportunities, the saturated zone of the Araba Formation, and the inferred faults affecting the subsurface sequence. Data of the vertical electrical sounding "VES" is obtained through the works of (Al-Abaseiry and Al Temamy 2012) and unpublished internal report of Desert Research Center (2019).

Table 2. Chemical analyses (major and trace) of the obtained groundwater samples, Wadi El Morra, South Sinai.

Major elements (mg/l)											
Well no.	pH	TDS mg/l	E.C. dS/m	Ca^{++}	Mg^{++}	Na^{+}	K^{+}	CO_3^{-}	HCO_3^{-}	SO_4^{-}	Cl^{-}
W7	7.16	593.00	1.08	11.50	45.36	125.12	36.00	0	70.00	122.06	218.00
W9	7.16	602.00	1.08	11.62	45.36	127.18	38.43	0	72.00	124.04	219.15
W11	7.91	892.14	1.49	42.69	1.58	247.24	74.51	0	126.91	176.44	287.23

Trace elements (mg/l)											
Well No.	Fe	Cu	Zn	Mn	Cd	Mo	Pb	Cr	Ni	NO_3	P_2O_5
W7	0.11	0.002	0.05	0.04	0.0003	0.0008	0.0007	0.012	0.001	0.02	0.14
W9	0.10	0.002	0.05	0.04	0.0003	0.0008	0.0007	0.012	0.001	0.02	0.14
W11	0.185	0.001	0.04	0.03	Nil	0.0002	Nil	0.020	0.001	0.04	0.15

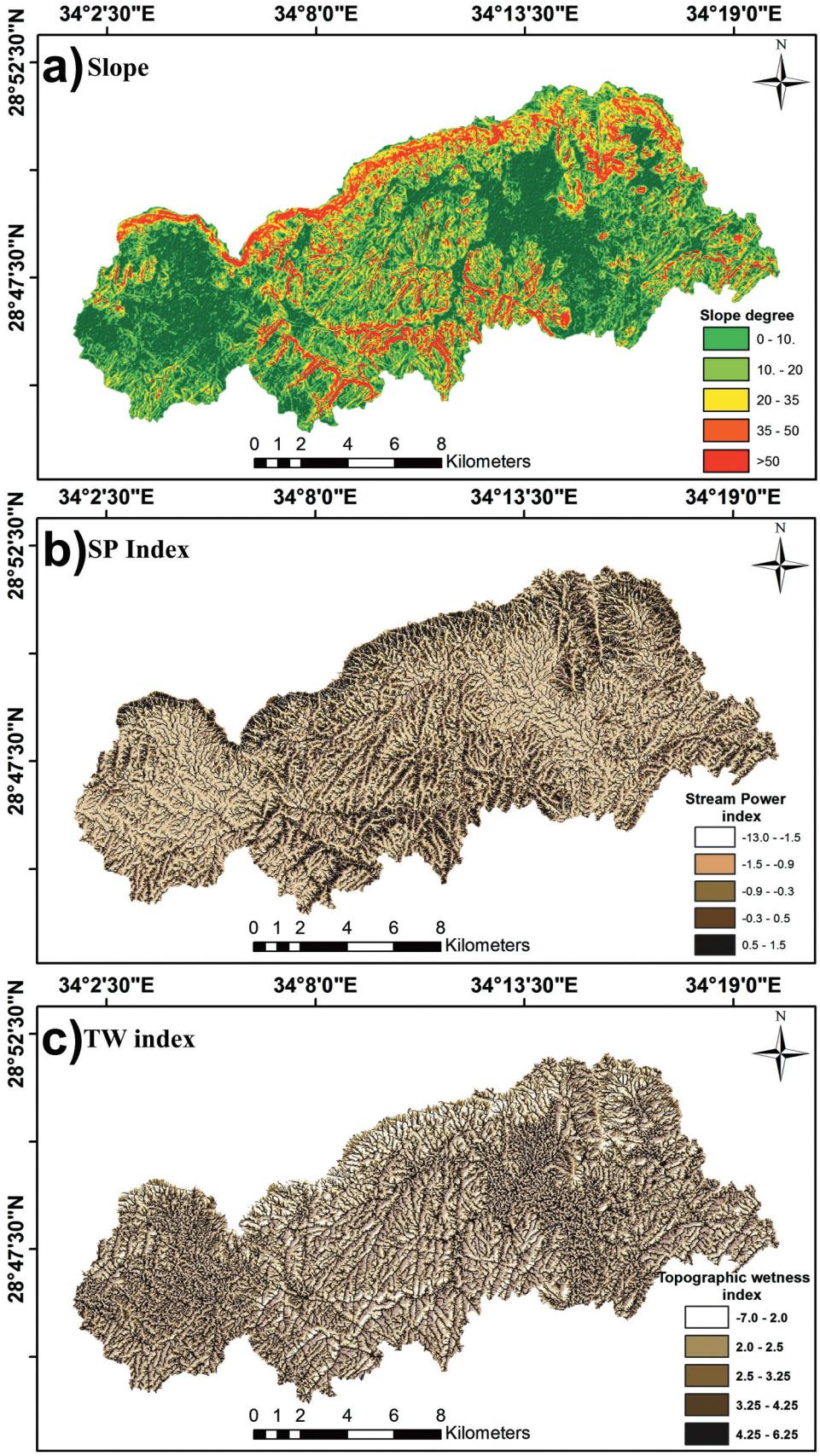

Figure 8. Thematic GIS data layers related to surface runoff of the studied basin. (a) Slope, (b) stream power index and (c) topographic wetness.

distribution of flora and fauna and its abundance (Moore et al. 1991; Wilson and Gallant 2000). Where, stream power index estimate the net denudation in areas of profile convexity (high flow acceleration) and net precipitation in locations of profile concavity (areas of low flow velocity). So the stream power index and erosion risk increase in catchment areas with high-profile gradient and

large upsloping contributing areas. In the current study, the calculated values of the SPI for El Morra basin are classified into five classes range between −13 to 1.5, (Figure 8(b)). The highest value of SPI means the higher possibility of erosive power and high flooding risk. Hence, pixels located within zone near from the road networks that have the maximum logarithm of SPI (−0.3–0.5; 0.5–1.5) values are expected to have the highest potential for flood risks.

4.4.3. Topographic wetness index (TWI)

TWI is an important index helps in illustrating the rainfall runoff patterns, through identifying areas of high potential soil moisture as well as ponding areas. Furthermore, TWI provides valuable information and assist in future development projects through the identification of areas susceptible to flooding (Masoud 2011; Ballerine 2017). This index is based mainly on the idea that the local slope and the upslope contributing area of certain points affects the soil moisture condition at this point. In the current study, the calculated values of the TWI for El Morra basin are classified into five classes range between −7 to 6.26, (Figure 8(c)). The highest value of TWI means the higher possibility of a land area to remain wet after flooding. Consequently, this could be possible measure recommended to recharge groundwater. Where, pixel sites near to the fault locations with high values of TWI (e.g. 3.25–4.25; 4.25–6.25) could be favourable location for potential recharging the groundwater aquifer in this location.

4.5. Rainfall analyses

Although Sinai Peninsula is classified as an arid land with limited water resources, it is frequently subjected to heavy storms leading to flash floods. The study area belongs to south Sinai district which subjected to many flood events due to the heavy rains and high mountains watersheds. The nearest meteorological station is present in Saint Catherin village which is so fare, the rainfall data was derived from the Global Rain Map (GSMAP) website[2]. The last hydrologic year extends from July 2018 to June 2019 was selected to investigate the response of El Morra watershed to the rainfall events occurred in this year. Six storms have been recorded (Table 3) where obtained data clarifies that the total amount of precipitation is about 217 mm. This year can be classified as a heavy rainy year compared with the average annual rainfall in the study area that attains 166.3 mm and the maximum daily rainfall reaches to about 37 mm in Saint Catherin station (Table 4). The collected storms were represented as hyetographs (Figure 9) which represents a plot of rainfall intensity against the time. The maximum rainfall intensity ranges from 3 mm/hr to 14.4 mm/hr where the total rainfall depths are ranging from 5.5 to 108.3 mm. According the hyetographs (Figure 9(a–f)), the storm of February 2019 constitutes the longest storm where it still rain about 43 hours during 5th and 6th of February while the storm of November 2018 represents the highest intensity storm (14.4 mm/hr) among the recorded storms.

4.6. Rainfall/runoff relationship

The SCS-CN method was applied to estimate Rainfall/Runoff relationship over El Morra basin. The most important parameter in this method is the accurate determination of the curve number (CN) value which depends on the soil group, land use and antecedent moisture content of the studied basin. El Morra basin was classified into three sub-basins (Figure 10) where the soil cover of each basin is identified regarding the geologic map and the field investigations. These soil categories range between hard basement rocks prevails the southern portion, sand soil (fine to coarse) dominates the middle part and lime soil presented in the north part (Figure 10). In addition, the basin area is proper bare area from cultivation & urbanisation and almost dry. Accordingly, the CN value of each soil category (Table 5) was obtained and the

Table 3. Different rainfall datasets of Wadi El Morra and Sinai.

The recorded storms in Wadi El Morra in the hydrologic year (July 2018 to June 2019)					
Storm	Storm day	Storm hour	Duration (hr)	Max. rainfall intensity (mm/hr)	Total rainfall depth (mm)
Sep. 2018	30	10–14, 19–23	10	5.5	13.1
Oct. 2018	25	03–06	4	5.2	5.5
Nov. 2018	14	11–22	12	14.4	36.3
Jan. 2019	27	02–13	12	7.7	39.7
Feb. 2019	5,6	12–06	43	8.5	108.3
Apr. 2019	8	04–12	9	3	14.5
Total					217.4

Source: https://sharaku.eorc.jaxa.jp/GSMaP/

Table 4. Annual & maximum rainfall in one day during 1976–2010 of the South and central Sinai meteorological station.

Meteorological station	Ras Sudr	Abu Rudeis	Al Tur	Sharm El Sheikh	Saint Catherin	Nuweiba	Taba	Nikhel
Annual rainfall (mm)	76.7	31.4	7.57	6.26	166.3	13.43	23.81	38.2
Maximum in one day (mm)	21.2	23.7	18.6	59	37.1	34.7	35.3	22.7

[2]https://sharaku.eorc.jaxa.jp/GSMaP/index.htm.

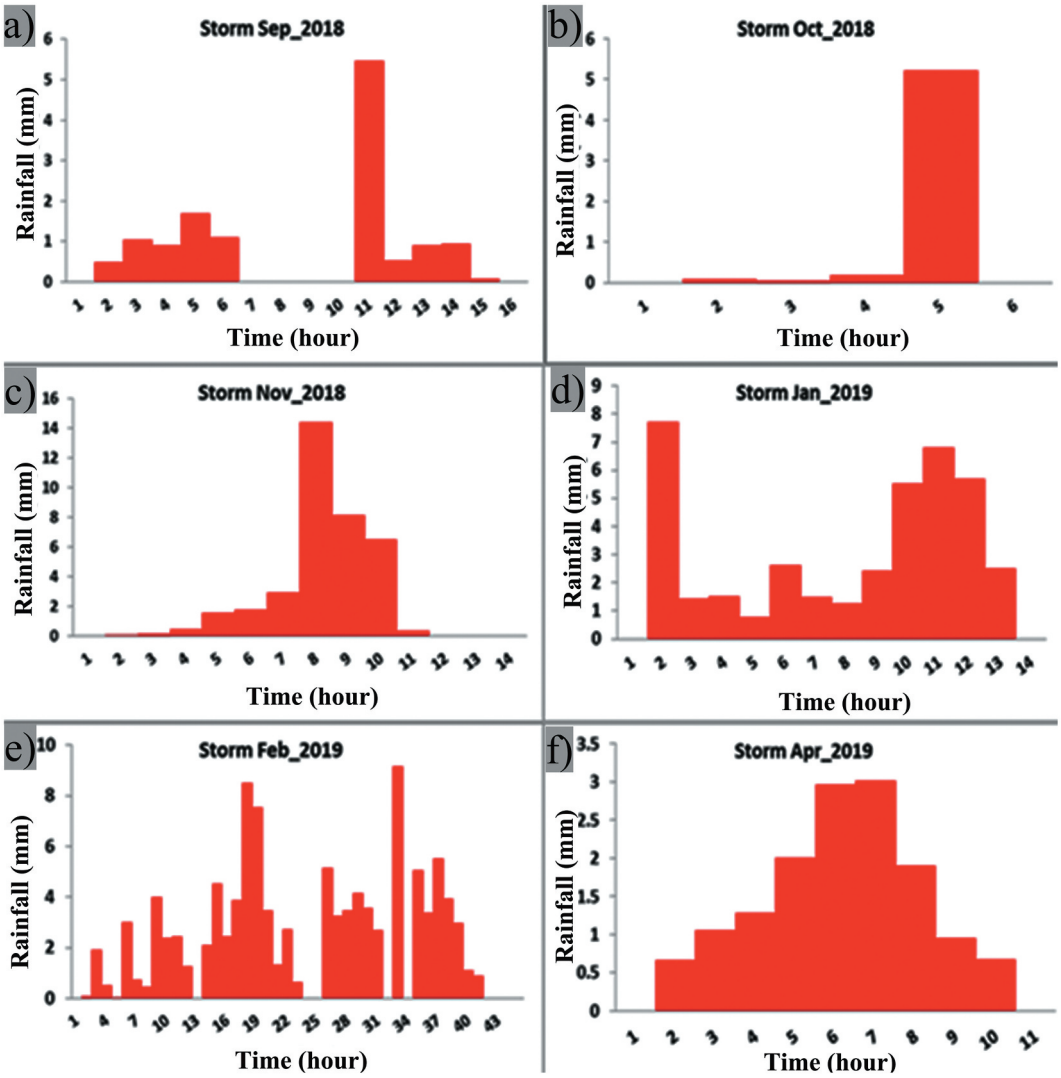

Figure 9. Storms hyetographs (a–f) recorded in the study area during the hydrologic year: July 2018 to June 2019.

estimated weighted CN values are ranging between 75 and 88. Accordingly, the initial abstraction (Ia) of El Morra basin ranges between 6.93 mm to 16.93 mm and the rainfall/runoff relation can be tabulated in (Table 5).

4.7. Runoff volume

The runoff volume of the un-gauged El Morra basin was estimated through the hydrograph generation using the HEC-HMS modelling software (V. 3.5) which was designed to simulate the precipitation/runoff process of the basin. The estimated values for time of concentration (Tc) range from 98 to 178 minutes and the lag time (T_L) range between 59 and 106 minute (Table 6). The output parameters of the HEC-HMS model include the hydrograph of the sub-basins at outlet point (Junction-2), the losses, peak discharge and runoff volume of the sub-basins (Figures 11 and 12(a–f), Table 7). The results reveal that the total runoff volume of the un-gauged El Morra basin in response of the six studied storm events, range from 0.377 to 18.088 $\times$ 10^6 m^3 with a total volume of 29.478 $\times$ 10^6 m^3 (represents 55.9% of the total rainfall over the basin) through the hydrologic year 2018–2019 (Table 7). The bulk quantity of this water was drained through the combined storm of February 2019 (18.088 $\times$ 10^6 m^3) where the storm extended for about 43 hr with maximum intensity of 8.5 mm and rain depth of 108.3 mm. On the other hand, the basin's peak discharge ranges between 69.1 m^3/s to 409 m^3/s. The storm of November 2018 recorded a very high peak (325.7 m^3/s) since this storm represents the highest rainfall intensity (14.4 mm/hr). The losses calculated in the different sub-basins reveal that the total losses amounts to 4.445 $\times$ 10^6 m^3 for sub-basin-1, 3.525 $\times$ 10^6 m^3 for sub-basin-2 and 15.207 $\times$ 10^6 m^3 for sub-basin-3 (Table 7). This is occurred due to the sandy nature of the sub-basin-3. The runoff coefficient can be identified as the relation between the runoff depth and rainfall depth that represents the amount of rainfall transmitted to runoff. The applying of Ponce's equations (1989) reveals that the runoff depths of El Morra basin under the different storms is ranging from 1.6 to 74.4 mm due to the difference between the

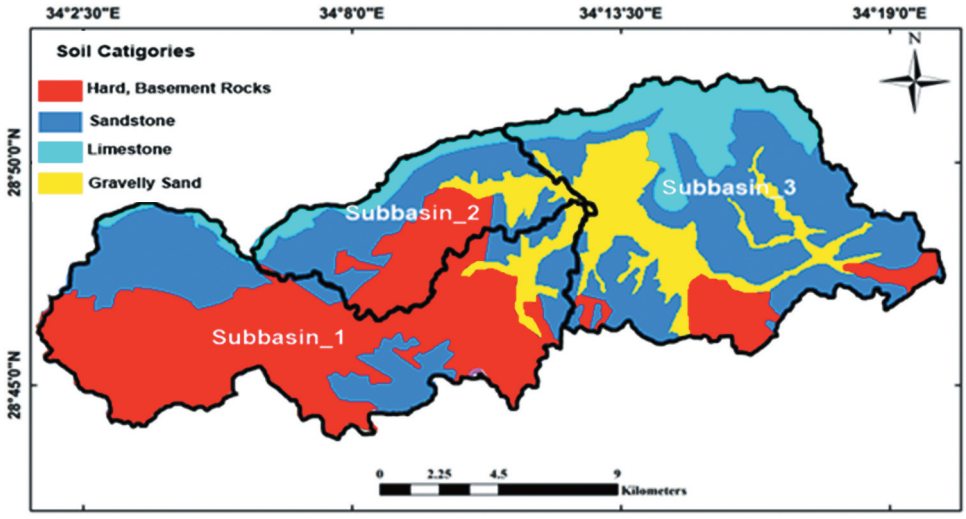

Figure 10. Soil categories map in Wadi El Morra basin.

Table 5. Rainfall/runoff relationship and results using SCS-CN method in Wadi El Morra (three subbasins).

Sub-basin	Area km^2	Land use	Soil type	Area Km^2	Cn	Weighted CN	S (mm)	Ia (mm)	Rainfall/runoff relation Q (mm)
Subbasin_1	104	Poor	D	78	91	88	34.6	6.9	$Q = (P - 6.9)^2/(P + 27.7)$
			B	21	81				
			A	5	72				
Subbasin_2	40		D	12	91	85	44.8	8.96	$Q = (P - 9)^2/(P + 35.8)$
			B	20	81				
			C	8	88				
Subbasin_3	99		A	79	72	75	84.6	16.93	$Q = (P - 16.9)^2/(P + 67.7)$
			C	15	88				
			D	5	91				

Table 6. Main inputs in HEC-HMS domain of sub-basins of Wadi Morra.

Basin name	Sub-basin	Impervious Ratio %	Losses Ia (mm)	Slope L (m/Km)	Time of concentration T_c (minutes)	Lag time (T_L) (minutes)
El Moraa basin	Subbasin_1	70	6.9	0.027	178	107
	Subbasin_2	30	8.96	0.04	98	59
	Subbasin_3	5	16.93	0.036	106	64

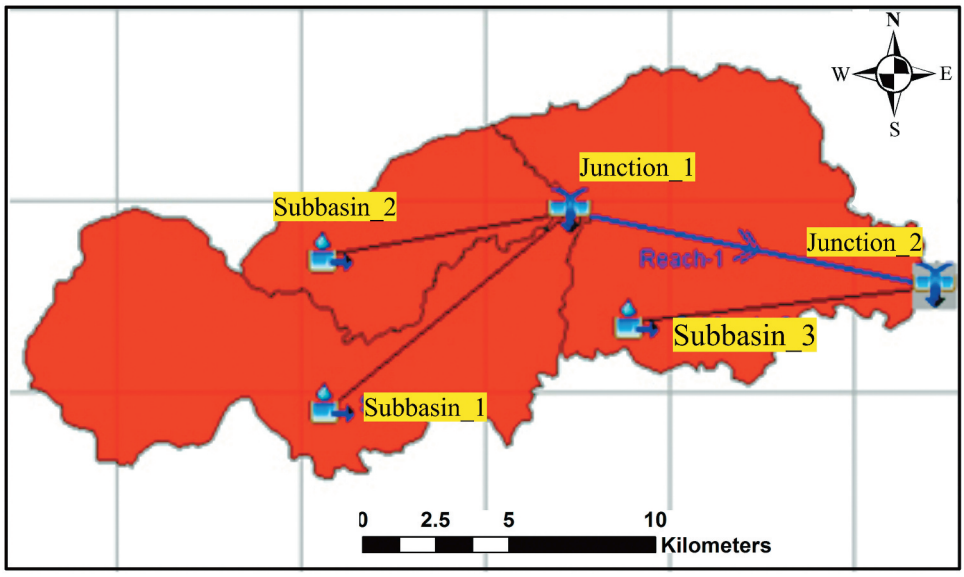

Figure 11. Wadi El Morra basin model domain.

magnitudes of the rainfall amounts (Table 8) while the estimated runoff coefficients range between 28.2% and 68.7%. The total loss of El Morra basin is estimated to about 23.177 × 10^6 m^3 (Table 9).

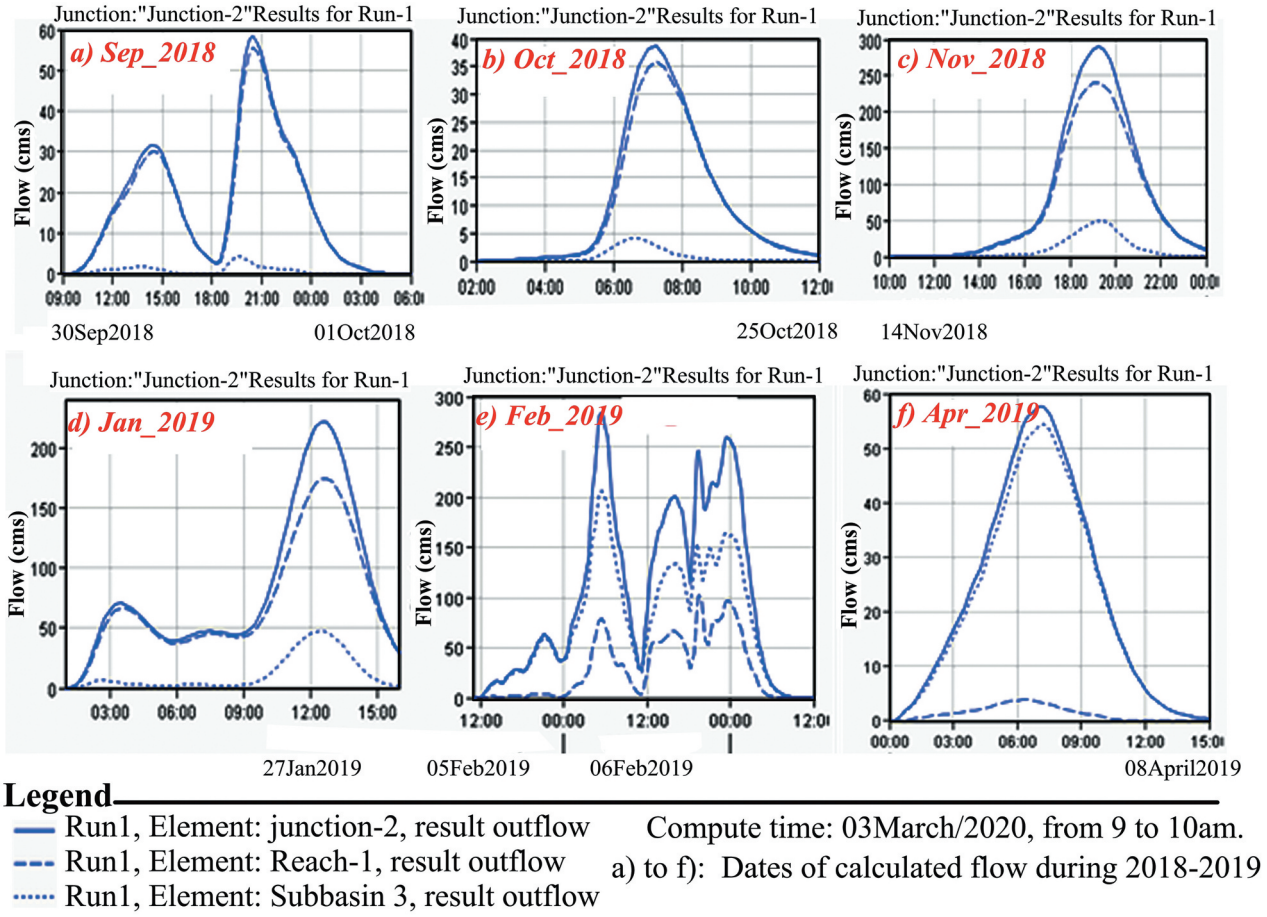

Figure 12. Direct runoff hydrographs of El Morra basin outlet with the different studied storms (a–f).

Table 7. Results of the hydrograph generation of El Morra basin with the different storms during the hydrologic year 2018–2019.

Parameters	Losses volume (m^3) × 10^6	Peak run-off (m^3/s)	Runoff volume (m^3) × 10^6	Losses volume (m^3) × 10^6	Peak run-off (m^3/s)	Runoff volume (m^3) × 10^6	Losses volume (m^3) × 10^6	Peak run-off (m^3/s)	Runoff volume (m^3) × 10^6
Storm		*Sep_18*			*Oct_2018*			*Nov_2018*	
Subbasin_1	0.315	48.4	1.042	0.287	29.3	0.287	0.949	187.1	2.785
Subbasin_2	0.359	11.4	0.167	0.156	10.7	0.067	0.731	57.2	0.729
Subbasin_3	1.232	4.3	0.065	0.520	4.1	0.027	3.078	48.6	0.517
Outlet		58.3	1.275		38.6	0.377		289.6	4.023
Storm		*Jan_2019*			*Feb_2019*			*Apr_2019*	
Subbasin_1	0.989	132.5	3.040	1.361	163.8	9.868	0.546	46.4	0.956
Subbasin_2	0.788	45.4	0.829	1.122	86.3	3.231	0.391	10.8	0.192
Subbasin_3	3.285	47.8	0.646	5.730	102.3	4.990	1.363	3.9	0.072
Outlet		221.8	4.496		284.3	18.088		57.7	1.219

5. Discussion

The basin under investigation, however it belongs to the hyper arid Sahara of Sinai, yet it receives seasonal flash flood events. This Sahara witnessed alternation from wet to dry periods during the last few million years (Abotalib et al. 2016, 2019a) and also throughout the wet periods the Saharan aquifers were recharged particularly in regions where the aquifer outcrops (as it was shown in Figures 4 and 7) are in contact with hydrographic basin outlets (Hussien et al. 2017; Yousif

Table 8. Runoff depth and coefficient values of El Morra basin.

Storm	Total losses (×10^6 m^3)	Peak discharge (m^3/s)	Runoff volume (10^6 m^3)	Runoff depth (mm)	Runoff coefficient (%)
Sep. 18	1.906	117	**1.275**	5.2	**40.1**
Oct. 18	0.963	75.1	**0.377**	1.6	**28.2**
Nov. 18	4.758	325.7	**4.023**	16.6	**45.6**
Jan. 19	5.062	241.6	**4.496**	18.5	**46.6**
Feb. 19	8.213	409	**18.088**	74.4	**68.7**
Apr. 19	2.3	69.1	**1.219**	5.0	**34.6**

Table 9. Total losses of El Morra watershed the sub-basins.

	Basin's losses $\times 10^6$ m^3 (hydrologic year 2018–2019) resulted from six storms						
Basins	*Sep-18*	*Oct_2018*	*Nov_2018*	*Jan_2019*	*Feb_2019*	*Apr_2019*	Total during hydrologic year
Subbasin_1	0.315	0.286	0.949	0.989	1.361	0.546	4.445
Subbasin_2	0.359	0.156	0.731	0.766	1.122	0.391	3.525
Subbasin_3	1.232	0.520	3.078	3.285	5.730	1.363	15.207
Total	1.906	0.962	4.757	5.040	8.213	2.300	23.177

et al. 2018). Therefore the extraction of the hydrographic basin (Figure 11) boundaries and their drainage networks (Figure 1) could indicate the potentiality of basin to harvest water throughout current and past pluvial seasons and show the capability of areas for groundwater recharge across surface runoff. The studied basin represents an example of structurally controlled terrain where tectonics play the main factor in groundwater occurrences. The tectonic structures have been influenced the subsurface sedimentary succession which is consequently affecting on the existence and potentialities of the aquifer. This can be clear when comparing between the setting of the dry wells and the productive wells (Figure 6). The results of band ratio calculation show that the sedimentary basin is existed in the northern portion of the basin while the southern side represents the basement uplift (Figure 5). Therefore, the Araba aquifer is existed in the northern portion with a saturated thickness ranges between 150 and 240 m while it is not recorded to the south of the main channel. This status is elucidated from the two hydrogeological cross sections (Figure 7) in comparison with the subsurface setting of the dry wells (Table 1). In addition, the extracted lineaments (joints and/or faults) indicate groundwater recharge opportunities through surface-groundwater interaction (Figures 6 and 7). Accordingly, the estimation of groundwater recharge was essential to evaluate the aquifer potentialities. The approach of determining the amount of recharged groundwater by using the initial and transmission losses under arid environments is a difficult issue due to the variability of surficial geomorphic characteristics (Figure 2) and infiltration capacities (Figure 10) of soils (Masoud 2011). The transmission losses in ephemeral channels are nonlinear functions of discharge and time (Lane 1972), and vary spatially along the channel reach and with soil antecedent moisture conditions (Sharma and Murthy 1994). The approach of Sorman and Abdulrazzak (1993) estimates that an average 75% of bed infiltration reaches to the water table where they applied an experimental research in Wadi Tabalah hyper-arid terrain (southwestern Saudi Arabia). The results of current study reveal that El Morra basin received a total 52.66×10^6 m^3 of rainfall (2018–2019) led to runoff volume about 29.47×10^6 m^3 and total losses amounts about 23.2×10^6 m^3 (Tables 6–9). Therefore, the expected amount of water recharged to the groundwater aquifer is estimated by 17.4×0^6 m^3 (represents 33% of the total rainfall over the basin) throughout the hydrologic year 2018–2019 (75% of the total losses). In addition, the extracted thematic layers include slope, stream power (SPI) and topographic wetness (TWI) indices reveal availability of basin flooding (Figure 8). The calculated values of the SPI are classified into five classes range between −13 and 1.5 where the highest value indicate the higher possibility of erosive power and high flooding risk. Also, the obtained TWI values of the TWI for El Morra basin are classified into five classes range between −7 and 6.26 where the highest values reveal the higher possibility of a land area to remain wet after flooding and consequently recharge the groundwater. Consequently, the investigation of these results clarified surface and groundwater potentialities of the studied basin where these water resources should be managed and exploited for different purposes. The current study approach approve that rainfall/runoff relationship is very important factor for the catchment management, i.e. sustainability of the water resources and protection from flood hazard. The obtained runoff values indicate that subbasin-1 has high tendency to runoff while subbasin-2 and subasin-3 have high susceptibility to recharge groundwater aquifers. Based on the mentioned hydrological parameters estimations for Wadi El Morra basin, an amount of 17.4×10^6 m^3 may recharge the groundwater aquifer through the modern precipitation (2018–2019) within this basin. This amount of annual recharge exceeds the annual extraction rates from the Araba sandstone aquifer, which was estimated as 0.35×10^6 m^3 (three productive wells are working with pumping rate: 320 m^3/8 h/day, Table 1). This significant contribution of modern recharge to the relatively shallow sandstone aquifer (belonging to Nubian sandstone system) demonstrates that the Araba sandstone aquifer in El Morra basin is renewable aquifer and can be recharged through the structural lineaments and also across the direct contact with its exposures. It is thought that the infiltrated modern water (e.g. 2018–2019 to the Araba aquifer mixes with the paleo waters that were precipitated during the Pleistocene wet climatic periods (Abotalib et al. 2019b)) and was reserved by the aquifer before it is ultimately drained into the Wadi Dahab mega-basin then to the Gulf of Aqaba. These results indicate that the aquifers existing in the structural controlled terrain receive topographically driven

annual recharge from sporadic and occasional rainfall events with significant amounts even under hyper-arid conditions.

5.1. Recommendation

Based on aforementioned results which reveal good potentialities of surface and groundwater resources, some recommendations are proposed for future exploration. The contribution of groundwater recharge to the Araba Sandstone aquifer can be artificially improved, using managed surface water harvesting (Missimer et al. 2015; Steinel et al. 2016). The volume of surface runoff to points which represent the outlets of the three sub-basins was estimated. Accordingly, the exploitation of the surface water can be achieved through establishing of artificial lake (Figure 13) to store some amounts of water and also enhancing the infiltration process to the Araba Sandstone aquifer. Reducing of the runoff flow velocity within sub-basins outlets through constructing of these lakes associated with alternative dams in front of lakes will accumulate surface water within the Wadi channels upslope and thus increasing the vertical head gradient. Based on the inspection of the high resolution satellite images (5 m Pixel, Microsoft hybrid image) and the results of hydrologic study (Figures 11 and 12), three locations were chosen as potential locations for lakes (L) (L1, L2 and L3, Figure 13) where they are characterised by: (1) suitable geological and topographic settings, (2) the Wadi channels are narrow, and (3) they are bounded by elevated basement terrains, (4) they receive a considerable amounts of surface water as indicated in Tables 6–9. These proposed lakes can also help to supply fresh water to the local communities for drinking and agriculture purposes. On the other hand, the groundwater exploration in the studied basin is so limited (only seven productive wells, Figure 6) while the obtained results reveal considerable annual amounts of rainfall can be infiltrated and recharge the groundwater (17.4×10^6 m^3 throughout the hydrologic year 2018–2019). Therefore, three proposed areas (G) are suggested for future exploration (G1, G2 and G3, Figure 13) through hydro-geophysical investigation and test wells drilling. These areas are determined according to their geological and subsurface setting where they are located in the sedimentary basin which expected to have thick thickness of sandstone belonging to Araba formation and can store water. Also, the three sites are representing the water collector area that has favourable conditions for recharge where they have low elevation and crossed by the main basin stream. The obtained chemical results (major and trace) show the low salinity of water without any heavy metal pollution, therefore, the exploration of groundwater can secure a good source for drinking purposes.

6. Conclusions

The current study introduces an integrated approach based on geological, hydrological and limited geophysical datasets, together with satellite imagery, to understand the groundwater conditions and its recharge opportunities in structurally terrain basin. The studied basin (El Morra) represents an example of structurally controlled terrain where tectonics have the main influence in groundwater occurrences. The tectonic settings and its related structural features have been affected the subsurface sedimentary succession which is consequently impacted on the existence and potentialities of the aquifer. This was very obvious when comparing between the geological setting of the dry and productive wells. The calculation of band ratio can be considered as a good tool which provides more information about the structural and geological setting. The hydrological analyses of this basin revealed that the estimated

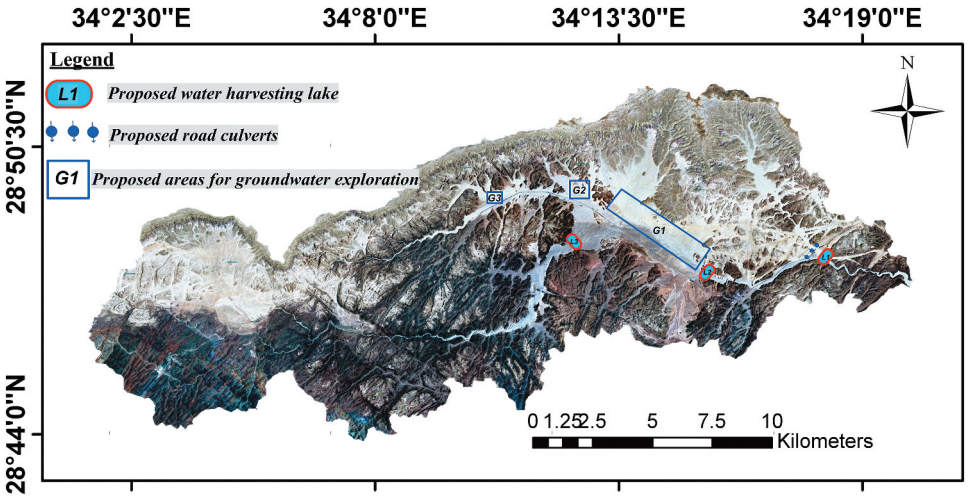

Figure 13. Recommendation map shows the proposed sites for surface water harvesting lakes and groundwater exploration. The sites are illustrated over a high-resolution Microsoft hybrid satellite image (5 m pixel resolution).

total losses amounts was about 23.2×10^6 m^3 where groundwater recharge reaches to 17.4×0^6 m^3 throughout the hydrological year 2018–2019. This amount of recharge that exceeds current annual extraction rates of Araba Sandstone (Cambrian) aquifer, representing a seasonal modern recharge to the aquifer. Therefore, the contribution of this modern recharge can be artificially improved using managed surface water harvesting. Accordingly, a total volume of annual harvested surface runoff estimated as 29.47×10^6 m^3 can be partly collected through three water harvesting lakes associated with alternative dams at the outlets of the sub-basins. Furthermore, the integration of remote sensing data sets together with hydrological and geological studies provides a comprehensive approach to explore factors controlling groundwater occurrences and its recharge in structurally controlled areas that suffering from data scarcity. Additionally, the integration of remote sensing data sets with GIS and field studies introduce a cost effective method in investigating the groundwater occurrences in desert areas, where it provide the accurate information about the best sites for drilling wells. Consequently, the absences of appropriate geological information in the study area led to the drilling of 4 dry wells as mentioned in section (5) which raised the cost of drilling groundwater wells. Moreover, the economic importance of such studies is to provide a source of fresh water supply for the locals depends on groundwater. Where, these groundwater wells could be the only option for local communities in desert area that secure the potable source of water.

Acknowledgements

The authors are grateful for Desert Research Center that provides all facilities to carry out the field trip and groundwater analyses of this research.

Disclosure statement

The authors approve that the current manuscript has no conflict of interest.

Funding

This research did not receive any specific grant from funding agencies in the public, commercial or not-for-profit sectors.

ORCID

Mohamed Yousif http://orcid.org/0000-0002-7847-9707

References

Abotalib AZ, Heggy E, Scabbia G, Mazzoni A. 2019a. Groundwater dynamics in fossil fractured carbonate aquifers in Eastern Arabian Peninsula: a preliminary investigation. J Hydrol. 571:460–470. doi:10.1016/j.jhydrol.2019.02.013.

Abotalib AZ, Sultan M, Elkadiri R. 2016. Groundwater processes in Saharan Africa: implications for landscape evolution in arid environments. Earth Sci Rev. 156:108–136. doi:10.1016/j.earscirev.2016.03.004.

Abotalib AZ, Sultan M, Jimenez G, Crossey L, Karlstrom K, Forman S, Krishnamurthy RV, Elkadiri R, Polyak V. 2019b. Complexity of Saharan paleoclimate reconstruction and implications for modern human migration. Earth Planet Sci Lett. 508:74–84. doi:10.1016/j.epsl.2018.12.015.

Adagunodo TA, Sunmonu LA, Oladejo OP, Ojoawo IA. 2013. Vertical electrical sounding to determine fracture distribution at Adumasun Area, Oniye, Southwestern Nigeria. J Appl Geol Geophys. 1(3):10–22. doi:10.9790/0990-0131022.

Al-Abaseiry AA, Al Temamy MA. 2012. Contribution of the geologic setting to the occurrence of groundwater in Wadi Morra, South Sinai, Egypt, Using geoelectrical techniques. Egypt J Geophys. 11:1–16.

Alnedawy F, Elnaggar AA, El-Mewafi M, Zeidan Z. 2015. Flood hazard evaluation and water harvesting estimation in South Sinai by using remote sensing and GIS techniques, case study (Dahab and Kid valleys). Int J Sci Eng Res. 6(7):1577–1583.

Arnous MO, Sultan YM. 2014. Geospatial technology and structural analysis for geological mapping and tectonic evolution of Feiran–Solaf metamorphic complex, South Sinai, Egypt. Arab J Geosci. 7(8):3023–3049. doi:10.1007/s12517-013-0959-5.

Ballerine C. 2017. Topographic wetness index urban flooding awareness act action support. Will & DuPage Counties (Illinois): Illinois State Water Survey.

Bentor YK. 1985. The crustal evolution of the Arabo-Nubian massive with special reference to the Sinai Peninsula. Precambrian Res. 28:1–74. doi:10.1016/0301-9268(85)90074-9.

Beven KJ, Kirkby MJ. 1979. A physically based variable contributing area model of basin hydrology. Hydrol Sci Bull. 24:43–69. doi:10.1080/02626667909491834.

Chow VT, Maidmen DR, May LW. 1988. In applied hydrology. New York: McGraw-Hill.

Das S. 2018. Geographic information system and AHP based flood hazard zonation of Vaitarna basin, Maharashtra, India. Arab J Geosci. 11(19):576. doi:10.1007/s12517-018-3933-4.

El Rayes A, 1992 Jan. Hydrogeological studies of Saint Katherine Area, South Sinai, Egypt [Master's Thesis]. Ismailia (Egypt): Suez Canal University.

El Shafei MK, Khawasik SM, El Ghawaby MA, 1992. Deformational styles in the tectonites of Wadi Sa`al area, South Sinai. Proc. 3rd Conf. Geol. Sinai Develop., Ismailia, Egypt. p. 1–8.

Eyal M, Eyal Y, Bartov Y, Steinitz G. 1981. The Tectonic development of the western margin of Gulf of Elat (Aqaba) rift. Tectonophysics. 80:39–66. doi:10.1016/0040-1951(81)90141-4.

Fishman MJ, Friedman LC, 1985. Methods for determination of inorganic substances in water and fluvial sediments. U.S. Geol. Surv. Book 5, chapter A1. Open File Report 85-495. Denver (Colorado).

Graf WL. 1988. Definition of flood plains along arid-region Rivers. In: Baker VR, Kochel RC, Patton PC, editors. Flood geomorphology. New York: Wiley; p. 231–242.

Hasanein AM. 2007. Comparative study of the effective geomorphologic and geologic features on the water resources in Wadis Baba and Dahab, South Sinai, Egypt. Sed Egypt Ain Shams Univ. 15:35–52.

HEC-HMS. 2010. Hydrologic modeling system HEC-HMS, version 4" US Army Corps of engineers, institute for water

resources. Davis (California): Hydrologic Engineering Center.
Hegazi AM. 2006. Tectonic evolution of the polydeformed Sa'al Belt, South Sinai, Egypt. Acta Geol Hungarica. 49/3:1–14.
Hussien HM, Kehew AE, Aggour T, Korany E, Abotalib AZ, Hassanein A, Morsy S. 2017. An integrated approach for identification of potential aquifer zones in structurally controlled terrain: Wadi Qena basin, Egypt. Catena. 149:73–85. doi:10.1016/j.catena.2016.08.032.
Japan International Cooperation Agency (JICA). 1999. Water Resources Research Institute (WRRI). South Sinai groundwater resources study in the Arab The Republic of Egypt; Main Report. Tokyo (Japan): Pacific Consultants International.
Kirpich A. 1940. Time of concentration of small agricultural watershed ASCE. Civil Eng. 10(6):1–362.
Klitzsch E, List FK, Pohlmann G. 1987. Geological map of Egypt, conoco coral and Egyptian General Petroleum Company, Cairo, Egypt, 2 Sheets. Scale. 1:500,000.
Lane LJ. 1972. A proposed model for flood routing in abstracting ephemeral channels. Hydrol Water Resour Ariz Southwest. 2(2):439–453.
Loizenbauer J, Wallbrecher E, Fritz H, Neumayer P, Khudeir AA, Kloetzli U. 2001. Structural geology, Single zircon ages, and fluid inclusion studies of the Meatiq metamorphic core complex implication for Neoproterozoic tectonics in the Eastern Desert of Egypt. Precambrian Res. 110:357–383. doi:10.1016/S0301-9268(01)00176-0.
Manoj G, Dholakia M. 2014. Impact of monthly curve number on daily runoff estimation for ozat catchment in India. Open J Mod Hydrol. 4:144–155. doi:10.4236/ojmh.2014.44014.
Masoud A. 2011. Runoff modeling of the wadi systems for estimating flash flood and groundwater recharge potential in Southern Sinai, Egypt. Arab J Geoscience. 4:785–801. doi:10.1007/s12517-009-0090-9.
Missimer TM, Guo W, Maliva RG, Rosas J, Jadoon KZ. 2015. Enhancement of wadi recharge using dams coupled with aquifer storage and recovery wells. Environ Earth Sci. 73(12):7723–7731. doi:10.1007/s12665-014-3410-7.
Moawad MB. 2013. Analysis of the flash flood occurred on 18 January 2010 in wadi El Arish, Egypt (a case study). Geomatics Nat Hazards Risk. 4(3):254–274. doi:10.1080/19475705.2012.731657.
Mohamed L, Sultan M, Ahmed M, Zaki A, Sauck W, Soliman F, Yan E, Elkadiri R, Abouelmagd A. 2015. Structural controls on groundwater flow in basement terrains: geophysical, remote sensing, and field investigations in Sinai. Surv Geophys. 36(5):717–742. doi:10.1007/s10712-015-9331-5.
Moore ID, Grayson RB, Ladson AR. 1991. Digital terrain modeling: a review of hydrological, geomorphological, and biological applications. Hydrol Process. 5(1):3–30. doi:10.1002/hyp.3360050103.
Muchingami I, Hlatywayo DJ, Nel JM, Chuma C. 2012. Electrical resistivity survey for groundwater investigations and shallow subsurface evaluation of the basaltic-greenstone formation of the urban Bulawayo aquifer. Phys Chem Earth Parts A/B/C. 50:44–51. doi:10.1016/j.pce.2012.08.014.
O'callaghan JF, Mark DM. 1984. The extraction of drainage networks from digital elevation data. Comput Vision Graphic Image Process. 28:323–344. doi:10.1016/S0734-189X(84)80011-0.
Omran A, Schroder D, El Rayes A, Geriesh M. 2011. Flood hazard assessment in Wadi Dahab Based on Basin Morphometry using GIS Techniques. GI_Forum Symposium and Exhibit applied Geoinformatics, Salzburg, Austria, Wichman, 1–11
Ponce VM. 1989. Engineering hydrology, principle and practices. Englewood Cliffs, N.J.: Prentice-Hall (New Jersy).
Rainfall data. 2018-2019. Global rainfall map (GSMaP) by JAXA global rainfall watch system (Ver. 4.0). Earth Observation Research Center, Japan Aerospace Exploration Agency. [accessed 2020 Mar 3]. https://sharaku.eorc.jaxa.jp/GSMaP/index.htm.
Said R. 1990. The geology of Egypt. A.A. Balkema: Rotterdam/Brookfield.
Sarikhani R, Kamali Z, Dehnavi AG, Sahamieh RZ. 2014. Correlation of lineaments and groundwater quality in Dasht-e-Arjan Fars, SW of Iran. Environ Earth Sci. 72(7):2369–2387. doi:10.1007/s12665-014-3146-4.
Shabana AR, 1999. Geology of water resources in some catchment areas drainage in the Gulf of Aqaba, Sinai, Egypt [Ph.D. Thesis]. Geol. Dept. Fac. Sci. Ain Shams Univ.
Sharma KD, Murthy JSR. 1994. Estimating transmission losses in an arid region. J Arid Environ. 26(3):209–219. doi:10.1006/jare.1994.1024.
Sharp IR, Gawthorpe RL, Underhill JR, Gupta S. 2000. Fault-propagation folding in extensional settings: examples of structural style and synrift sedimentary response from the Suez rift, Sinai, Egypt. Geol Soc Am Bull. 112(12):1877–1899. doi:10.1130/0016-7606(2000)112<1877:FPFIES>2.0.CO;2.
Shimron A. 1984. Metamorphism and tectonics of a Pan African terrain in southeastern Sinai, a discussion. Precambrian Res. 24:173–188. doi:10.1016/0301-9268(84)90057-3.
Soil Conservation Service "SCS". 1972. Estimation of direct runoff from storm rainfall, National engineering handbook. Section 4-hydrology, Washington DC,USA; p. 10.1–10.24.
Solomon S, Quiel F. 2006. Groundwater study using remote sensing and geographic information systems (GIS) in the central highlands of Eritrea. Hydrogeol J. 14(6):1029–1041. doi:10.1007/s10040-006-0096-2.
Sorman AU, Abdulrazzak MJ. 1993. Infiltration-recharge through wadi beds in arid regions. Hydrol Sci J. 38(3):173–186. doi:10.1080/02626669309492661.
Steinel A, Schelkes K, Subah A, Himmelsbach T. 2016. Spatial multi-criteria analysis for selecting potential sites for aquifer recharge via harvesting and infiltration of surface runoff in north Jordan. Hydrogeol J. 24(7):1753–1774. doi:10.1007/s10040-016-1427-6.
Sultan M, Metwally S, Milewski A, Becker D, Ahmed M, Sauck W, Soliman F, Sturchio N, Yan E, Rashed M, et al. 2011. Modern recharge to fossil aquifers: geochemical, geophysical, and modeling constraints. J Hydraul Eng. 403(1–2):14–24. doi:10.1016/j.jhydrol.2011.03.036.
UNESCO. 1979. Map of the world distribution of arid regions: map at scale 1: 25,000,000 with explanatory note. MAB technical notes 7. Paris: UNESCO.
Walters MO. 1990. Transmission losses in arid region. J Hydraul Eng. 116(1):129–138. doi:10.1061/(ASCE)0733-9429(1990)116:1(129).
Wilson JP, Gallant JC, eds.. 2000. Terrain analysis: principles and applications. New York, NY: John Wiley & Sons.
World Health Organization (WHO). 2014. Guideline for drinking water quality. 3rd ed. Vol. I recommendations. Geneva, ISBN 97892 4 154815 1. https://www.who.int. Accessed 4 Dec 2019.

Yousif M, Henselowsky F, Bubenzer O. 2018. Palaeohydrology and its impact on groundwater in arid environments: Gebel Duwi and its vicinities, Eastern Desert, Egypt. Catena. 171:29–43. doi:10.1016/j.catena.2018.06.028.

Yousif M, Hussien HM. 2020. Flash floods mitigation and assessment of groundwater possibilities using remote sensing and GIS applications: Sharm El Sheikh, South Sinai, Egypt. Bull Natl Res Cent. 44:50. doi:10.1186/s42269-020-00307-x.

Yousif M, Sracek O. 2016. Integration of geological investigations with multi-GIS data layers for water resources assessment in arid regions: El Ambagi Basin, Eastern Desert, Egypt. Environ Earth Sci. 75(8):684. doi:10.1007/s12665-016-5456-1.